Manuscript <u>±</u>

The Cyclotron Gas Stopper at FRIB getting ready for operations

S. Schwarz^{a,*}, C. Sumithrarachchi^a, G. Bollen^{a,b}, C. Magsig^a, D. J. Morrissey^{c,d}, J. Ottarson^c, A. C. C. Villari^a

^aFacility for Rare Isotope Beams, FRIB, East Lansing, MI, USA
^bDepartment of Physics and Astronomy, Michigan State University, East Lansing, MI,

USA

^cNational Superconducting Cyclotron Laboratory, NSCL, East Lansing, MI, USA ^dDepartment of Chemistry, Michigan State University, East Lansing, MI, USA

Abstract

Linear gas stopping cells have been used for nearly two decades to slow down projectile fragments at the National Superconducting Cyclotron Laboratory, now the Facility for Rare Isotope Beams, for experiments with low-energy and reaccelerated beams. In order to efficiently stop and rapidly extract light to medium-mass fast ions, a cyclotron gas-stopper has been constructed. It uses a cyclotron-type magnet and a helium-gas filled stopping chamber to slow down the injected beam. RF ion guides transport the stopped ions to the center of the magnet and axially through the bore before acceleration to <60 keV.

Following successful offline tests, the cyclotron stopper was moved to an experimental vault and connected to a new momentum-compression beam line. Beam transport to and into the cyclotron stopper was tested with stable beams. Using ⁴⁶K fragments, the first successful stopping and extraction of a high-energy beam with the cyclotron stopper was demonstrated.

Keywords:

Gas stopping, Radioactive beams, Cyclotron

Email address: schwarz@frib.msu.edu (S. Schwarz)

Preprint submitted to Nuclear Instruments and Methods in Physics Research BFebruary 24, 2023

^{*}Corresponding author.

1. Introduction

Gas stopping of energetic projectile fragments has been an important pathway to science with unique stopped and reaccelerated beams at the National Superconducting Cyclotron Laboratory (NSCL). The NSCL has transitioned into the Facility for Rare Isotope Beams (FRIB) in order to create significantly more exotic and more intense beams, prompting novel upgrades to the gas-stopping facility. FRIB will continue to operate linear gas-stopping cells to provide projectile fragments at low energy [1, 2]. In order to extract the lightest ions rapidly, which do not stop efficiently in linear gas cells due to their limited stopping lengths, a gas-filled reverse cyclotron has been constructed. A device based on this concept has been used to slow down and trap exotic light particles at LEAR/CERN [3] and it was proposed for the slowing-down of very light ions [4].

Developing this concept further [5, 6], the FRIB cyclotron gas stopper uses a cryogenic helium-gas filled stopping chamber inside a superconducting cyclotron-type magnet with a maximum field strength of $\approx 2.6\,\mathrm{T}$ [7] to confine the injected beam and bring it to a near halt. Degraded to a magnetic rigidity adequate for the field strength at the entrance radius of the stopping chamber, ions spiral towards the center of the device as they decelerate in the buffer gas. Traveling-wave RF ion carpets [8, 9], sized to cover the expected stopping distribution from combined LISE++/Monte-Carlo-type stopping simulations [6, 10], take the ions to the center of the device. There, an ion conveyor [11] extracts them at low gas pressure through the magnet bore out of the cyclotron stopper. The spiral deceleration path provides one to two orders of magnitude larger stopping length compared to linear gas stoppers that operate at similar gas pressure while keeping the travel and extraction times similar.

2. Offline commissioning, preparation of high-energy vault

For construction and low-energy ion transport tests, the cyclotron stopper was initially installed at a location separated from the NSCL high-energy beam lines. The magnet and related cryogenic infrastructure were commissioned and the magnetic field distribution at the nominal excitation current of 180 A demonstrated [12]. With the magnet operational, the low-energy ion guides were tested with an internal test ion source. Efficient ion transport along the ion carpets and the ion conveyor were demonstrated with and without the magnet energized [13].

While the low-energy ion transport tests were progressing, a dedicated high-energy vault was prepared to house the cyclotron stopper. Given the magnet's weight of $\approx 170\,\mathrm{tons}$, concentrated on a small area, a part of the vault floor had to be replaced and reinforced using micropiles to provide a solid foundation. In parallel, planning and construction progressed for a new momentum-compression line to connect the cyclotron stopper to the A1900 fragment separator. Similar to the beam lines for the linear gas stoppers, the new line features a copy of a 45-degree dipole used in the A1900 fragment separator and two large-bore magnetic triplets. They disperse the beam at a wedge degrader while focusing the momentum-compressed beam into the cyclotron stopper.

Figure 1 shows COSY beam calculations for the dispersive horizontal plane with three beams: one with a nominal rigidity of 3 Tm and two more with $\pm 1.25\%$ relative momentum deviation dp/p. The calculated momentum dispersion from the degrader location to the wedge position near the end of the beam line is 14.4 mm per percent dp/p.

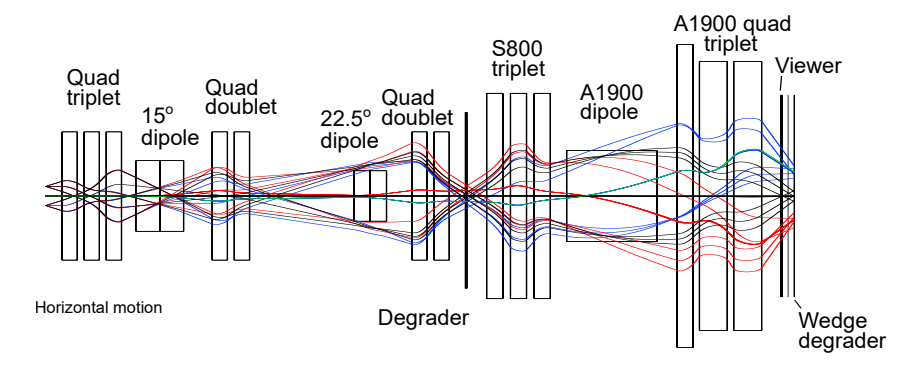


Figure 1: Calculated beam transport from the A1900 focal plane through the new momentum compression line to the wedge degrader box at the entrance of the cyclotron stopper. The three beams have a nominal rigidity of $3\,\mathrm{Tm}$ and $\pm 1.25\,\%$ dp/p in the dispersive horizontal plane.

3. Commissioning the momentum compression line

In 2018-19 the cylotron stopper was disassembled, moved to its online location in the so-called N2/3 vault and the momentum-compression line was completed. Figure 2 shows a photograph of the vault taken near the end of construction.

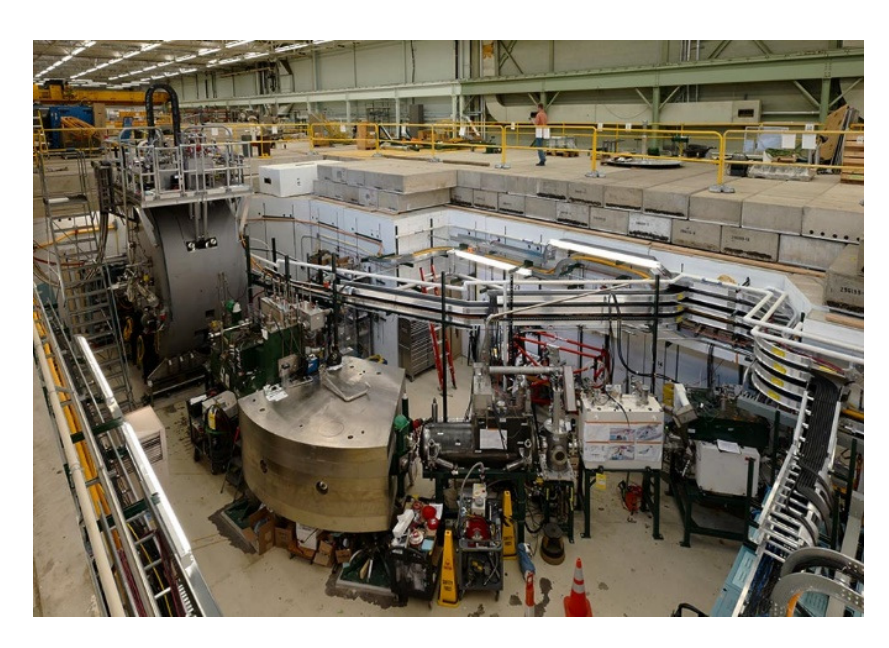


Figure 2: Photograph of the N2/3 vault with the new momentum-compression beamline and the cyclotron stopper.

The new beamline was commissioned in two runs in 2019 with primary ⁴⁰Ca and ⁴⁸Ca beams, confirming beam optics calculations. Commissioning the cylotron stopper with high-energy beam started in 2020 with primary ⁷⁸Kr and ⁴⁸Ca beams. In all tests with primary beams the rate sent into the N2/3 vault was limited by discarding the dominantly fully-stripped primary beam on a beam blocker and transmitting a small H-like fraction through the A1900. A thin scintillator at the A1900 focal plane was used to monitor the beam rate. After passing through that scintillator most of the beam sent into the N2/3 vault was fully-stripped, while a small fraction remained H-like. During the run with ⁷⁸Kr beam an Al plate with effective thickness of 1168 um was installed at the degrader position indicated in Figure 1 to reduce beam rigidity to 2.14 Tm prior to injection into the cyclotron-stopper. As shown in Figure 3, three beam spots were observed on a viewer installed at the wedge location. LISE++ calculations, based on COSY optics input are shown on the right of the Figure. They indicate that the three beam spots are compatible with charge states 35+ and 36+, obtained by charge exchange in the scintillator at the A1900 focal plane and the degrader, and

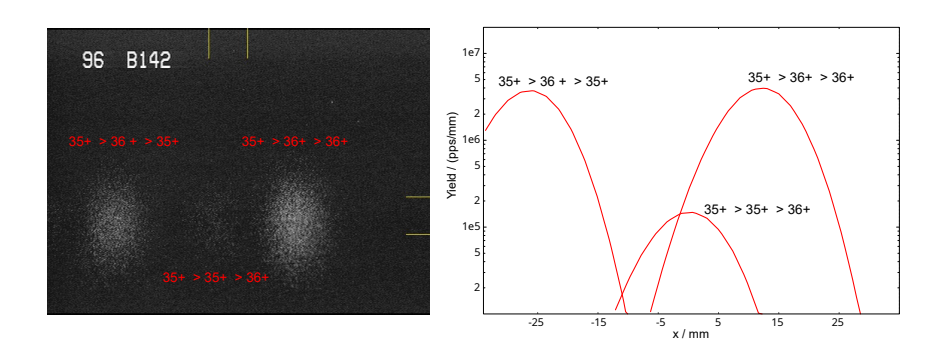


Figure 3: Left: beam image recorded at the last beam viewer of the N2/3 momentum-compression beam line. The image shows three beam spots, compatible with charge states 35+ and 36+ of $^{78}{\rm Kr}$ beam, obtained by charge exchange in the scintillator at the A1900 focal plane and an Al degrader. Right: LISE++ calculation showing the expected positions for the three beams at the viewer.

the expected momentum dispersion of the line.

4. Injection tests

For the commissioning runs with the cyclotron stopper, two Si detectors were installed inside the stopping chamber, shown in Figure 4. The first one is located at the edge of the last degrader and can rotate into the beam path when the degrader is not in use. The second detector is mounted on a movable arm to probe the radial beam distribution 240° behind the last degrader.

Figure 5 shows two radial ⁴⁸Ca beam distributions recorded with the second detector while the stopping chamber was evacuated and filled with 100 mbar He gas, respectively. With the chamber evacuated and the final degrader reducing beam rigidity to match the magnetic field strength at the degrader radius, the injected beam will perform a near-circular motion outside the detector range. For the scan without gas, the degrader was set to a lower rigidity with most of the beam circulating at large radius. As eccentricity increases at lower rigidity with larger degrader angles, more beam penetrated into the detectable range and led to the detected profile expected from the simulations at that degrader angle.

Using 100 mbar of He gas, the now inward-spiraling motion led to a peaked profile at minimum degrader angle. The simulations indicate a larger angle would have shifted the maximum to a smaller-than-detectable radius.

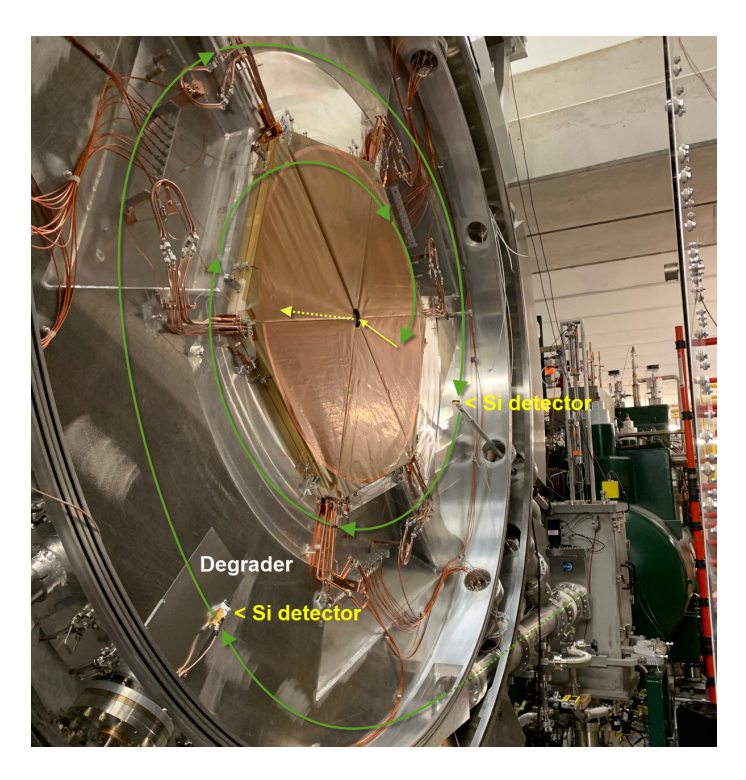


Figure 4: Photograph of the interior of the stopping chamber. The large RF carpets (copper color), the degrader plate, and the two Si detectors are visible in the image. A schematic path of the beam passing the final degrader, spiraling to rest above the carpet is indicated in green and the path of the ions across the carpet to the center and exiting through the bore is indicated in yellow.

5. Stopping and extraction test with ⁴⁶K

Efficient stopping and transport along the ion carpets requires a He gas pressure of a few tens of mbar, while the ion conveyor inside the magnet bore works best at a few mbar before beam is extracted to vacuum; see [13] for details about the ion guide setup. Pumping equipment similar to that in use for FRIB's linear gas stoppers was added to provide the necessary differential pumping. A third Si detector was installed at the end of the ion conveyor to record extracted beam.

A beam of 46 K fragments, obtained from a 48 Ca primary beam, was sent into the momentum compression line with ≈ 2.6 Tm rigidity. It was degraded further to ≈ 1.1 Tm by a 2.5 mrad-angle wedge degrader, two Al beam win-

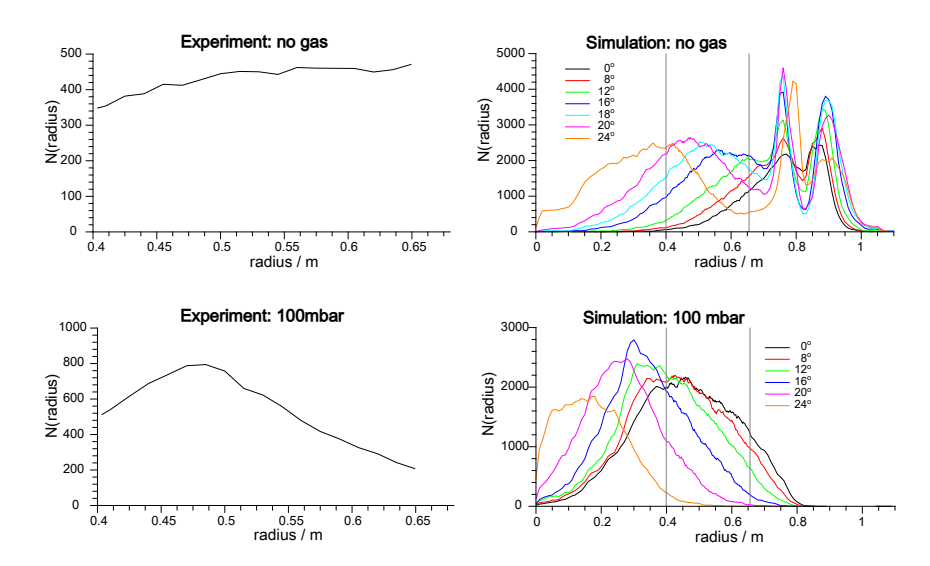


Figure 5: Radial detector scans. The left two panels show experimental count rate as a function of radial detector position with the chamber evacuated (top) and filled with 100 mbar He (bottom). The right panels show corresponding simulations, performed for different final degrader thicknesses, labeled by rotation angle. The vertical lines in the right panels mark the range of detector movement.

dows with a combined thickness of 177 um and the rotatable 508 um degrader inside the stopping chamber. The rigidity was chosen to match the magnet's excitation at 96 A, which resulted in $\approx\!79\%$ of the maximum field strength. Ions came to rest in helium gas at up to 47 mbar pressure. The large ion carpets shown in Fig. 4 were operated near 7.5 MHz and 96 V $_{pp}$ RF amplitude, while the conveyor was driven with an 8-phase square RF voltage of $50\,\mathrm{V}_{pp}$ at 3 MHz. Beta activity with a half-life of $^{46}\mathrm{K}$ was detected at the end of the ion conveyor, which proved successful extraction of this beam from the cyclotron stopper.

Figure 6 (left) shows the negative ionization current recorded with the plates providing the pushing field of the carpets inside the stopping chamber, as well as ion current and beta count rate at the detector behind the ion conveyor. For this test the chamber pressure was 47 mbar, while the conveyor pressure was near 8 mbar. Maximum beta count rate was observed for a large degrader angle at low ionization current. Corresponding stopping simulations for these conditions agree with the findings that efficient stopping of ions happens at large degrader angle, when ionization is concentrated near the

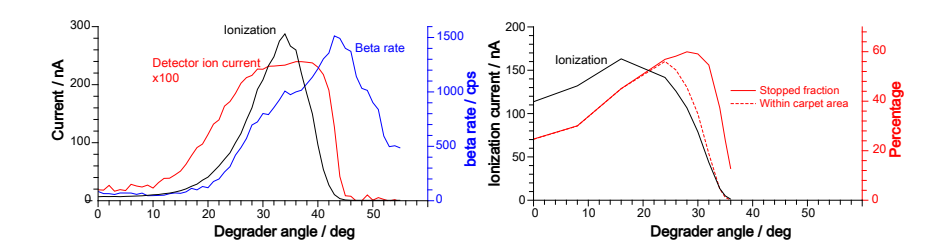


Figure 6: Degrader scan from extraction tests with 46 K. Recorded quantities in the experiment (left) include the ionization current in the carpet volume, beta count rate and the current observed at the Si detector at the exit of the cyclotron stopper. Simulated quantities shown on the right: ionization current, fraction of injected beam stopped inside the stopping chamber and within the carpet radius of $0.44\,\mathrm{m}$.

degrader and low inside the carpet area. The transmission of ⁴⁶K beam from the A1900 focal plane to the last detector behind the conveyor was in the one-percent range observed in these initial time-limited tests. The tests were cut short by the transition of the NSCL facility to FRIB. One can expect that the efficiency will be considerably improved with further testing and optimization, since FRIB recently has started operations.

6. Outlook

Following the successful extraction tests, plans are progressing to connect the cyclotron stopper to an expanded FRIB stopped-beam distribution area. The area will include a high-resolution mass separator complementing the existing but relocated separator and integrate a high-current EBIS charge breeder [14].

Acknowledgements

This material is based on work supported by the National Science Foundation under Grant Nos. PHY-09-58726, PHY-11-02511 and PHY-15-65546 as well as support from Michigan State University. This material is based upon work supported by the U.S.Department of Energy, Office of Science, Office of Nuclear Physics and used resources of the Facility for Rare Isotope Beams (FRIB), which is a DOE Office of Science User Facility under Award Number DE-SC0000661.

References

- [1] K. Lund et al., Nucl. Instr. Methods B463 (2020) 378–381.
- [2] C. Sumithrarachchi et al., Nucl. Instr. Methods B463 (2020) 305–309.
- [3] L. Simons, Physica Scripta T22 (1988) 90–95.
- [4] I. Katayama et al., Hyperfine Interactions 115 (1998) 165–170.
- [5] G. Bollen et al., Nucl. Instr. and Meth. A550 (2005) 27.
- [6] N. Joshi et al., in: Proceedings of IPAC 2012, New Orleans, USA, jacow.org, p. TUPPR087.
- [7] S. Chouhan et al., IEEE Trans. Appl. Supercond. 23 (2013) 4101805.
- [8] G. Bollen, Int. Journal of Mass Spectrometry 299 (2011) 131.
- [9] M. Brodeur et al., Int. Journal of Mass Spectrometry 336 (2013) 53.
- [10] O. Tarasov, D. Bazin, Nucl. Instr. Methods B376 (2016) 185–187.
- [11] A. Colburn et al., Physics Procedia 1 (2008) 51–60.
- [12] S. Schwarz et al., Nucl. Instr. Methods B376 (2016) 256–259.
- [13] S. Schwarz et al., Nucl. Instr. Methods B463 (2020) 293–296.
- [14] H.-J. Son et al., J. of Physics: Conf. Series 2244 (2022) 012018.

Declaration of interests ☑ The authors declare that they have no known competing financial interests or personal relationships that could have appeared to influence the work reported in this paper. ☐ The authors declare the following financial interests/personal relationships which may be considered as potential competing interests: